THE UNIVERSITY OF QUEENSLAND

Bachelor of Engineering Thesis

PRACTICAL LIMITATION OF GRID-CONNECTED LITHIUM-ION BATTERY

Student Name: Gde Ngurah Renaldi Shantika

Course Code: MECH4501

Supervisor: Dr. Ruth Knibbe

Submission Date: 30 May 2019

A Thesis submitted in partial fulfilment of the requirements of the

Bachelor of Engineering degree in Mechanical & Mining Engineering

UQ Engineering
Faculty of Engineering, Architecture and Information Technology

Acknowledgements

This thesis was done under the support of the School of Mechanical and Mining Engineering of the University of Queensland and people who encouraged me throughout the 1 year of the thesis project execution.

First of all, I would like to thank my thesis supervisor, Dr. Ruth Knibbe for her guidance and countless constructive advice for me to great through many obstacles. I am very grateful for every meeting session which were being held for consultation and knowledge sharing.

Furthermore, I would also want to thank Ben Spencer for providing me with some information about grid services and Yuriz Mayolie for thoroughly proof-reading the report.

Abstract

The vast development of lithium-ion batteries (LIB) has gained a lot of interest from many researchers. The particular improvement of LIB research is that LIB is starting to be used in a grid system called battery energy storage system (BESS). This thesis project aims to determine what type of LIB is suitable to be used in different grid systems. To choose which type of LIB that is suitable for the system, the cycling efficiency and the degradation mechanism of the LIB must be studied. Currently, the types of LIB used for BESS are Lithium Iron Phosphate (LFP) and Lithium Nickel Manganese Cobalt (NMC). Despite the capability of LFP and NMC, their degradation mechanism is still an essential part of the limitation of the BESS. Additionally, the degradation of LFP and NMC are affected by temperature and current rate (C-rate) such that increasing both parameters will result in higher degradation. The variation of temperature and C-rate proves that LFP has superior stability compared to NMC, despite having lower capacity than NMC. Therefore, it can be concluded that LFP is more suitable for a high cycling system while NMC is more suitable for system which has high capacity storage as their primary concern.

Table of Contents

List of Figures

List of Table

1. Introduction

The high energy density and good recharge capability of lithium-ion batteries (LIB) have driven rapid LIB development over the past decades. LIBs are often used in portable electronic devices, power electronics, electric vehicles, and for grid-connected energy storage.

The LIB is typically categorized according to the cathode chemistry. The most common chemistries are Lithium Nickel Manganese Cobalt (NMC), Lithium Iron Phosphate (LFP), Lithium Manganese Oxide (LMO) and Lithium Cobalt Oxide (LCO). LCO cathodes are commonly used for mobile phones, laptops and other digital devices [1], while LFPs and NMCs are popularly used for electric vehicles (EV) [2]. Additionally, LFPs and NMCs are currently being developed for energy storage of grids such as Battery Energy Storage System (BESS) [3]. NMC has the most attractive cathode chemistry as it provides a longer battery life compared to other types of LIB, however new battery chemistries are continuously being developed to improve the LIB capacity, efficiency and long-term stability. In particular, long-term stabilities are crucial for the utilisation of LIB in BESS. The focus of this thesis will be around the long-term stability of the LIBs.

Although BESS is not as significant as the current energy storage system (ESS), it is predicted that BESS will have a major improvement in the upcoming years due to its unique advantages. To increase the performance of BESS, characteristics of LIB are studied further. There are several parameters that require fulfilment in order to obtain optimal performance from a BESS. The active degradation mechanism is the first to consider when selecting LIB for BESS due to its significant effect on battery performance. Despite showing good performance for energy storage, LIB degradations have been the main cause of its poor adoption for BESS in Australia.

Among the factor that could affect the degradation mechanism, temperature is a major factor. As stated by the Australia Government Bureau of Meteorology, Australia has a mean temperature of 30 °C, which is close to the LIB optimal operating temperature. While this is the case, Australia is expecting an increase of average temperature in the upcoming years, with prediction of hotter extremes [4]. This could adversely affect the interest of using LIB as battery energy storage system. As the average temperature of Australia increases, the inflation of degradation in performance of LIB will occur. Therefore, LIB with a higher stability is necessary to be developed to withstand the extreme condition in Australia.

Due to this reason, LIB degradation studies have become an increasingly important topic. Increasing the cycle and calendar life would have a dramatic cost implication for companies

interested in purchasing large banks of LIBs. While there are numerous LIB degradation mechanisms, only the critical degradation mechanisms that will need to be considered.

LIB can degrade even when not in use, but this degradation is small compared to the degradation which occurs during battery cycling. As such, it is crucial to obtain an understanding LIB cycling degradation which in some documentation is referred to as aging on cycling. Based on literature findings, LIB degradation not only depends on the battery chemistry, but also the condition under which the battery is used. The key controlling parameters of LIB degradation are temperature, current density and cut off voltages.

According to Birkl, et al. [5], the degradation mechanism can be divided into 3 groups - Loss of Lithium Inventory (LLI), Loss of Active Material of Negative Electrode (LAM_{NE}) and Loss of Active Material of Positive Electrode (LAM_{PE}).

Most LIBs studies are mainly aimed at their performance for electric vehicle (EV) storage. However, as the LIB industry grows, further research is required to understand the LIBs' performance when used in other applications – such as grid-connected energy storage. NMC and LFP are the most commonly-used LIBs for grid energy storage. Therefore, this thesis will focus on obtaining a deeper understanding of the degradation in these systems. More specifically, this thesis will look into the grid-connected LIB services and the impact on battery degradation. This work will be supported by conducting an extensive literature review on grid-connected LIBs and the LIB degradation mechanism.

2. Objectives

The main goal of this thesis project is to understand how different operating condition affect the degradation of LIB performance, such that a suitable LIB can be chosen for utilisation in multiple grid usage in Australia. To achieve this goal, this thesis is broken into several key tasks, which are:

1. Understand the operation of LIB;
2. Examine specific chemistry of NMC and LFP batteries;
3. Understand and review the main services grid-connected LIBs provide;
4. Review and assess the key degradation mechanisms for LIBs with a focus on NMC and LFP batteries; and
5. Understand the impact of the grid-connected LIB operating conditions on LIB degradation.

3. Literature Review

Nowadays, renewable energy has gained increasing interest as an energy supply. The common storage system used is called energy storage system (ESS). Due to limitation of ESS technology, the development of battery energy storage system (BESS) is starting to rise. BESS, as it is named, utilises a rechargeable battery such as LIB for energy storage. This storage system currently contributes to 10% of the total of energy storage system share and expected to increase to 25% per annum from 2011 to 2021 [5]. Despite holding only, a small share, BESS has a massive total battery capacity of about 11 GWh (2017) and predicted to increase to between 100 GWh and 167 GWh (2030). This increase is caused by strong aspects of BESS which are very fast response time, low self-discharge, high efficiency and feasibility of scaling due to modular structure [3].

There are various services of grids such as stationary energy storage and frequency regulator. As the name says, frequency regulator functions to control the frequency in a power system. Due to the inverse proportionality of frequency and load in the system, any increase in load will lead to the slowing down of frequency. Therefore, a certain amount of power burst is needed to counteract the frequency variations. These are when BESS are needed because of its fast response during under frequency and its ability to store more power during over frequency events [6]. In comparison, stationary energy storage only has the amount of energy stored as the primary concern, thus the system will need LIB with higher battery capacity.

According to Hesse, et al. [3], the parameters for LIB selection that will be used in battery energy system storage;

- Safety and maturity on battery cell level;
- Degradation and aging mechanism;
- Power capability;
- Cycling efficiency and self-discharge;
- Energy contents of the battery cell; and
- Material and battery cell cost.

3.1. Lithium-Ion Battery (LIB)

Lithium-Ion Battery (LIB) is one of the most popular rechargeable batteries. It is different to normal batteries in that the chemical reactions occurring in the rechargeable batteries are reversible, this will be explained further in the next section. Lithium (Li) is a light metal with the highest electrochemical potential and can produce the highest specific energy for a battery. However, the development of lithium batteries is halted due to its safety problems, which is why lithium ions are used for rechargeable batteries instead. Compared to lithium metal, lithium ion forms a low maintenance battery and is considered safer. In contrast to its lower energy density compared to lithium metal, lithium ions' energy efficiency is significantly higher than both nickel-metal hydride batteries [7]. Despite the benefits of lithium ions, LIBs are fragile and have active degradation mechanisms, with the latter resulting in decay of battery capacity.

3.1.1. How the Battery Works

The operation of LIBs is illustrated in Figure 1.

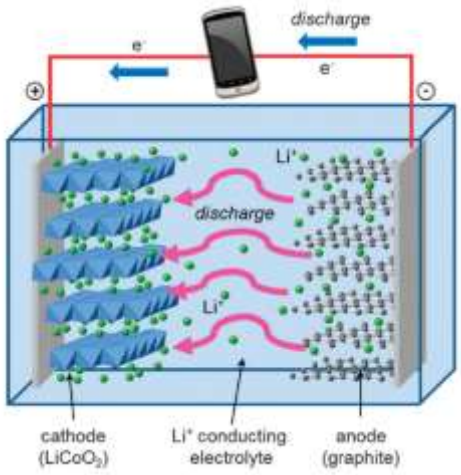

Figure 1 Discharging of LIB [8]

As a rechargeable battery, LIB experiences two processes: charging and discharging. During discharge, the lithium ions move from positive electrode (cathode) to negative electrode (anode) through a separator and electrolyte. The cathode will experience reduction or gain of electrons while the anode will experience oxidation or loss of electrons. As the electrons moving from anode to cathode, a useful power is produced for battery-connected devices. The reverse reaction occurs for charging process. During charging, a voltage is applied across the electrodes such that the lithium ion will move back from the cathode to anode, intercalating between the graphite layer of the anode.

3.1.2. Components of LIB

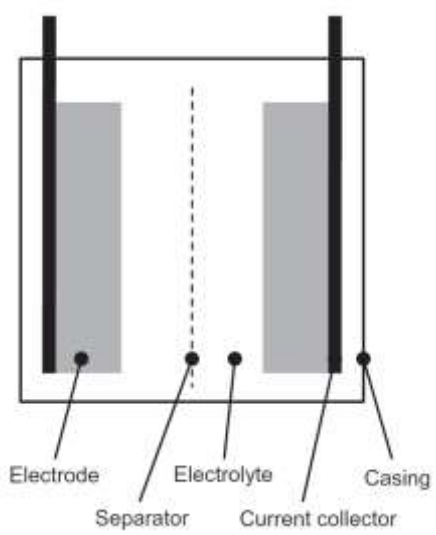

Figure 2 Component of LIB [9]

As shown in Figure 2, the typical construction of LIBs is made of electrodes (cathode and anode), separator, electrolyte, current collector, and casing. These components can be divided into active and non-active components. Active components are those involved with the reduction-oxidation (redox) reaction of the battery (electrodes), with the rest being non-active components are not involved to redox (separator, electrolyte, current collector, and casing) [9].

Electrodes

The electrodes are the most important LIB component as they contain the active components for the Li oxidation and reduction processes. For these reactions to occur, it is essential that the electrode materials are porous and have good electrical and ionic conductivity [10]. The materials which are commonly used for anode is titanium oxides and graphite. These materials are preferred due to exhibiting relatively little structural change during intercalation and deintercalation of lithium ions (volume expansion of graphite is 11%) [11]. This is important because the minimum structural change result in high stability of the anode. However, carbon is more popular due to economic and technical reasons. For the cathode, lithium insertion materials such as NMC, LFP, and LCO. are common [9].

Separator

The main function of the separator in LIB is to prevent direct contact between the cathode and anode. Without the separator, the contact between these electrodes would lead to a short circuit. Furthermore, the separator must be porous to ensure the Li migration between the electrodes. An effective separator will require pore sizes of <1 µm, thickness of 20 – 25 µm, and porosity of 40% to 60% [12].

Improved performance is exhibited with the use of a tri-layered separator Polypropylene-Polyethylene-Polypropylene (PP/PE/PP) due to its strength and thermal stability. This layered structure also causes the separator to act as thermal fuse protection of LIB [12]. This occurs at the time of overheat or overcharge, as PE melts and cause the pores to close, preventing any lithium ions to pass through. . For this reason, PP/PE/PP performance is dependent on the low melting point of PE and high melting point of PP. However, the thermal fuse function of the

separator can be enhanced by coating the PP/PE/PP separator with thermoplastic ethylene-ethyl acetate copolymer microspheres [12].

Electrolyte

In LIB, electrolyte is a solution composed of the combination of one or more salts which dissolved in one or more solvents [9]. The electrolyte plays an important role in making sure there is free flow of lithium ions between electrodes to generate electricity. Foremost, the electrolyte must be stable and compatible with the electrodes to allow efficient charging and discharging. Furthermore, it is essential that the conduction of ions through the electrolyte is rapid enough to prevent redox reaction from occurring. Liquid electrolyte typically has high ionic conductivity, but relatively low mechanical strength. In contrast, solid and polymer electrolytes are more flexible in format (to obtain higher mechanical strength), but has lower ionic conductivity [9].

Electrolyte is involved in the formation of the solid electrolyte interphase (SEI) on the anode surface [13]. The formation of SEI layer depends on the electrolyte used in the LIB, therefore the composition of electrolyte used is essential for the LIB structure. The most common electrolytes solvents used for LIB are ethylene carbonate (EC), dimethyl carbonate (DMC), diethyl carbonate (DEC), and ethyl methyl carbonate (EMC) and lithium hexafluorophosphate ($LiPF_6$) as the electrolyte salt. Nowadays, some LIBs utilise a mixture of these electrolyte solvents to improve optimal performance of the battery [14].

Current Collector

A current collector is used to collect or supply electrons to the electrodes. To do this, it is crucial that the current collector has a good electrical conductivity. Hence, it is usually made of copper and aluminium as they are known to have high conductivity. Aluminium is commonly used for the cathode, while copper is used for the anode [15]. In addition, the current collector also needs to be stable especially within the electrochemical environment. It is desirable that the current collector does not take part in cell redox reaction [9].

Casing

The casing benefits the battery by limiting outside influence on the cell. This results in cells stability as the outside environment prevented from disrupting the battery's operation. If the cells are not protected with a proper casing, it might lead to rupture, leakage or even explosion [15].

3.2. Types of LIB Cathode

Promising outlooks are observed for the use of lithium insertion materials for LIB cathode. This is due to the fact that electrochemical insertion and deintercalation are essential for battery performance and lithium insertion material takes a big part on it. Furthermore, good ionic and electronic conducting materials are key to faster charging and discharging processes. Thus, lithium insertion materials such as LMO, NMC, LFP, and LCO are suitable for better performance of LIB [11]. The difference between these materials is that each provide a different capacity value and stability for the LIB. In particular, NMC and LFP shows the highest potential in its utilisation for LIBs due to capacity and cycling stability.

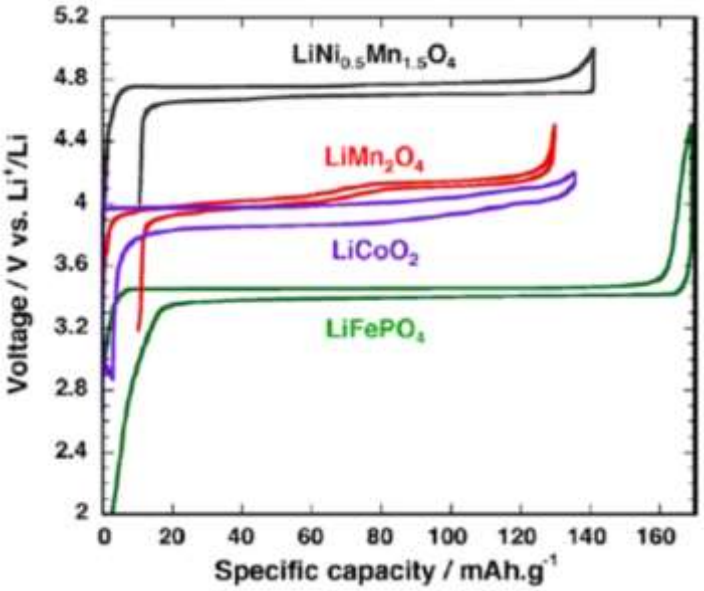

Figure 3 Comparison of Charge and Discharge Curve for Each Different Cathodes [11]

3.2.1. Lithium Nickel Manganese Cobalt (NMC)

In the crystal structure of NMC ($LiNi_xMn_yCo_{1-x-y}O_2$) crystal structure, the cobalt ions are trivalent (Co^{3+}) , whereas manganese ions are tetravalent (Mn^{4+}), and nickel ions are divalent (Ni^{2+}). NMC possess a complex structure, especially its cationic order which has purpose to minimise strains between the larger (mainly Ni^{2+}) and smaller ions (mainly Mn^{4+} and Co^{3+}). During charging, the Ni^{2+} are oxidized into trivalent, Ni^{3+} (stable) and tetravalent state, Ni^{4+} (unstable), whereas Co^{3+} are oxidised into tetravalent state, Co^{4+} [11]. In literature, the development of NMC materials is to maximise the benefits of each transition metals (Ni, Mn, and Co). For example, higher composition of nickel will result in higher capacity, but at cost of safety characteristic. On the other hand, high composition of cobalt and manganese shows improved cycling and safety characteristic, but at cost of capacity. Therefore, it is suggested that an optimum composition of the three transition metals are used to build NMC to manifest every aspect of benefits from each metal [16].

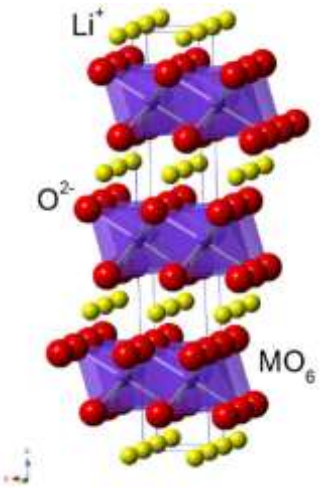

Figure 4. Crystal Structure of NMC [56]

As stated on the previous section, researchers are trying to develop higher capacity materials such as $LiNi_{1/2}Mn_{3/2}O_4$. However, after testing it, $LiNi_{1/2}Mn_{3/2}O_4$ shows low stability despite having high capacity of 230 mAh/g [17]. This low stability is caused by the presence of Mn^{3+} in the structure at charge state. To achieve LIB with a stable cell at high capacity, NMC or $LiNi_xMn_yCo_zO_2$ is one of the solutions. The insertion of cobalt transition metal reduces the amount of Mn being oxidise to Mn^{3+} state [9].

In addition, it must be kept in mind that the composition optimisation of NMC is essential for better LIB performance. Currently there are several compositions of NMC that are developed and researched. These compositions are NMC333, NMC442, NMC532, NMC622, and NMC811. There are a lot more variance of NMC composition being researched, but the afore-mentioned are currently the common types of NMC for LIB cathodes. A research by Ma, et al. [19] shows that at voltage of 4.2 V, the NMC811 has specific capacity of 215 mAh/g, the highest compared to other types of NMC. The high Ni content of NMC811 has great contribution to this high capacity. However, it also results in lower content of Mn and Co, reducing the stability of the material. From the research, it is concluded that the amount of Mn^{4+} has substantial impact on the thermal stability of NMC because it is not electrochemically active [18].

Equally important is the choice of electrolytes in producing an optimal performance. Genieser, et al., conducted an experiment in which different composition of electrolytes with additives were used to analyse NMC333 performance. Ethylene carbonate (EC) and ethyl methyl carbonate ethyl methyl carbonate (EMC) are used as the main electrolyte in this experiment. On the other hand, vinylene carbonate (VC), prop-1-ene-1,3-sultone (PES), 1,5,2,4-dioxa-dithiane 2,2,4,4-tetraoxide (DTD) and tris-trimethylsilyl-phosphite (TTSPi) are used for additives for the electrolytes. This experiment shows that, NMC 333 works the best with electrolyte composition of EC: EMC (3:7) with additives of 2% PES, 1% DTD and 1% TTPSi. With this electrolyte and additive composition, NMC333 is found to produce the best cycling stability at 55°C and capacity loss of about 3.6%. However, after cycling at 80 °C, the battery did not experience any crystalline structural changes as predicted [19]. This experiment highlights the importance of electrolyte optimisation on battery performance. However, the topic of electrolyte optimisation is out of the scope of this thesis project due to lack of systematic data that this report covers.

3.2.2. Lithium Iron Phosphate (LFP)

LFP or $LiFePO_4$ has an olivine structure which is made up of FeO_6 octahedra and PO_4 tetrahedra that are linked by corners and edges [11]. The olivine structure is reported by Goodenough and co-workers and it is adopted from the orthorhombic space group Pnma in 1990 [17]. In the crystal structure of LFP, lithium ions occupy the interstitial void available. An in-situ X-ray is able to show two distinct phases on the LFP structure, triphylite and heterosite.

$$LiFePO_4\ (triphylite)\ \leftrightarrow FePO_4\ (heterosite) + Li^+ + e^-$$

Initial report on LFP shows poor capability and low utilisation of the battery even at low C-rates. This is behind the reason of low electrical conductivity of the triphylite and heterosite phase. One proposed answer to this problem is the use of carbon coating by inserting carbon materials during initial synthesis. This solution brings the beneficial effect of delaying the grain growth of the material, producing small particles that allow rapid release of lithium ions [17].

According to Padhi et al., $LiFePO_4$ and $FePO_4$ have similar structures. The small difference between both structures eliminate the possibility of crystal structure damage. Due to the small decrease in volume about 6.81% and also the increase in density about 2.59%, the LFP has excellent stability [20]. This olivine structure of LFP gives better stability, thus prolonging the lifespan of the battery. Nevertheless, LFP still has lower voltage compared to other cathode materials.

With the mechanism and structures complexity of LFP, the material holds its own benefits and drawbacks. An optimized LFP can deliver capacity close to the theoretical capacity of about 170 mAh/g even at higher C-rates which is favourable for LIB performance. Furthermore, LFP structure has strong P-O covalent bonds, creating delocalized chemical bond which makes the cathode thermally stable even at high temperature of 200 °C [21]. Despite its benefits, LFP still has a low working potential which is responsible for the limited energy of LIB.

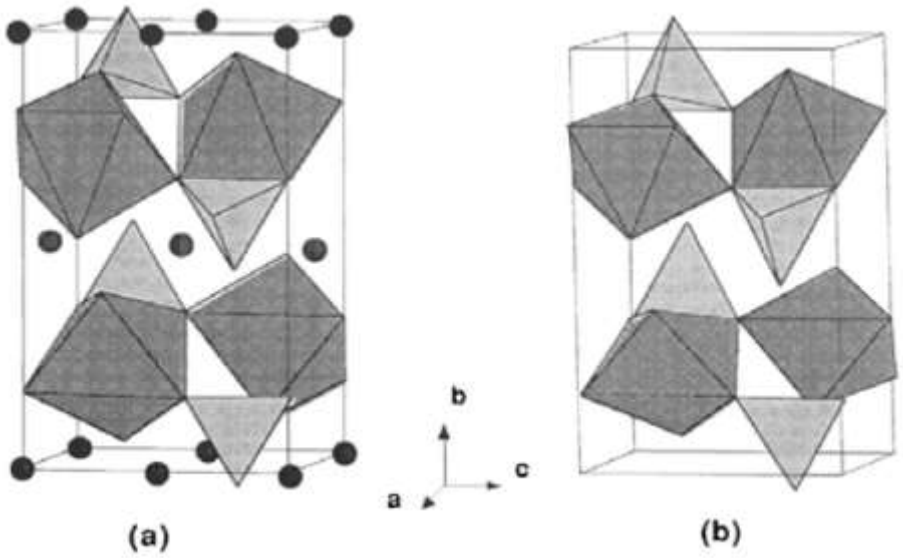

Figure 5 Crystal Structure of (a) $LiFePO_4$ and (b) $FePO_4$ [21]

To obtain a desirable LIB, a compatible electrolyte and cathode is necessary. $LiPF_6$ is a popular salt for the battery's electrolytes, but its lack of stability results in the formation of hydrofluoric acid which accelerate dissolution of iron in the positive electrode. On the contrary, LiODFB provides stable SEI films and therefore can compete with other low temperature electrolyte. For the electrolyte solvents, EC, EMC and diethyl carbonate (DEC) are most commonly used [21].

Shavora et al. proved that long term cycle of LFP is more compatible with using Li-imides salts as its electrolyte additives. Compared to VC, Li-imides salts such as LitFSI lead to much smaller capacity fades of about 2% at 20 °C. With the presence of imide salts, the SEI layer produced is also thinner, consist of more LiF and has lower resistance compared to when VC is used [22]. This is important because higher resistance of SEI layer will cause slower diffusion of lithium ion into the electrodes or out of the electrodes which is unfavourable.

3.3. Types of LIB Anode

The anode of LIB is as significant as the cathode in determining the performance of a battery. Many chemical reactions occur in the anode, amongst them is the decomposition of electrolyte due to the potential difference produced during lithium insertion. This decomposition can result in SEI formation which could lead to battery performance degradation. Furthermore, like the positive electrode, anode with high stability must be used in order to ensure battery's safety.

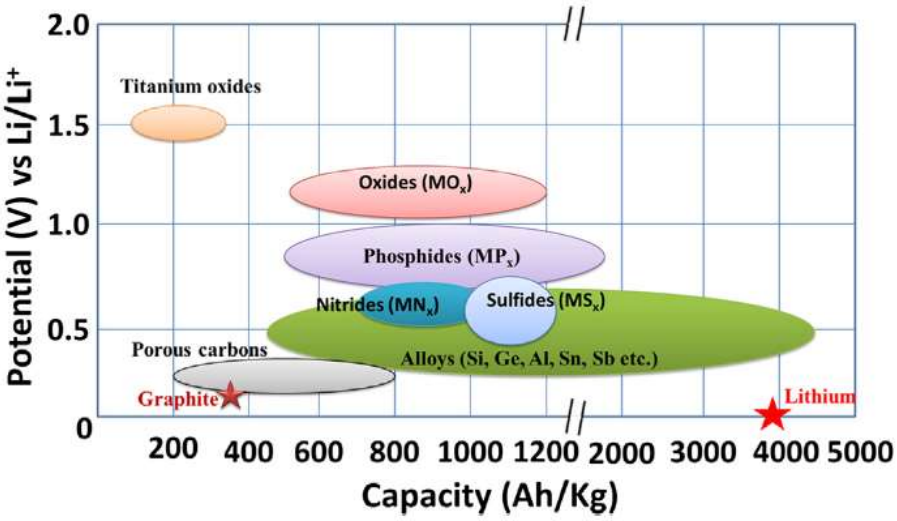

Figure 6 Comparison of Possible Anode Material for LIB [23]

3.3.1. Carbon

Out of many anode materials, carbon is the most widely used material for LIB anode. This is due to its low working potential, low cost of carbon, high reversibility, and stability in chemical, thermal and electrochemical environment. The most stable type of carbon is graphite. Graphite's redox potential is close to lithium ions, which is the reason behind the stability of graphite for LIB anode [24]. Despite its stability, using carbon as anode for LIB also has its drawbacks such as for most intercalation of lithium ions, it is resulted by stoichiometry of LiC_6 which has lower energy capacity than the desired ones (372 mAh g^{-1}) and low energy density [25]. In some conditions, lithium salt ($LiPF_6$) may also react with moisture and form HF which causes surface corrosion of the electrodes. This could result in slow degradation and formation of SEI layer on anode. This could be prevented by coating the anode using carbon that act as HF corrosive resistance [23]. As continuous intercalation of lithium occurs on the anode during charging, the capacity of the LIB will decrease. This is due to volume expansion on the graphite anode, occurring especially at higher C-rates.

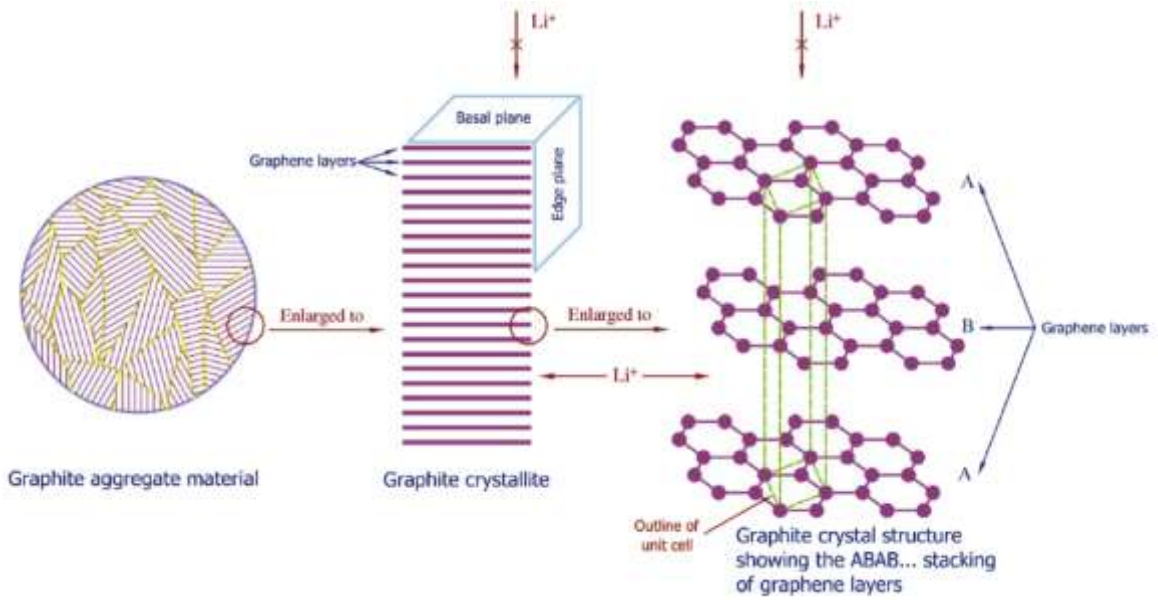

Figure 7 Illustration on Lithium Ion Intercalation Process into and Out of Graphite Anode [24]

3.3.2. Titanium Oxides

One of the types of titanium oxides that is used as LIB anode, also one of the best choice of anode material, is lithium titanite or LTO ($Li_4Ti_5O_{12}$). In LTO, the lithium insertion occurs at a much higher potential compared to graphite, thus, reducing the decomposition of the electrolyte which could lead to SEI formation. The superiority of LTO is also behind the reason that LTO experience low volume expansion (about 0.2%) during charging or discharging [26]. However, LTO still has low electric conductivity compared to graphite and during cycling, LTO produces gasses (hydrogen and CO_2) which leads to loses in capacity which are not preferable for the LIB performance [11]. For this reason, LTO will require further research and development before it is able to replace graphite as the choice of anode material.

3.4. Battery Testing

In the operation of LIB, the performance of LIB is determined by several factors such as the voltage of the battery and current rates. These factors might lead to either greater performance of LIB or the degradation of its performance.

3.4.1. Charging and Discharging

A full cycle of battery operation normally consists of two states which are the charging state and discharging state. In a full cell where it is connected to a load, electrons will flow from anode to cathode through the load, leading to reduction reaction in the cathode materials and oxidisation reactions in the anode. During electron flow, anions (negative ions) and cations (positive anions) will be transferred to the anode and cathode respectively [15]. This process is what is called as discharging. On the other hand, during charging or recharge state, the electron flow is reversed. In charging state, oxidation occurs on the cathode while anode is reduced. This means that the anode is now considered as positive electrode while the cathode is the negative electrode. The electrochemical operation of discharge and charge are illustrated by Figure 8.

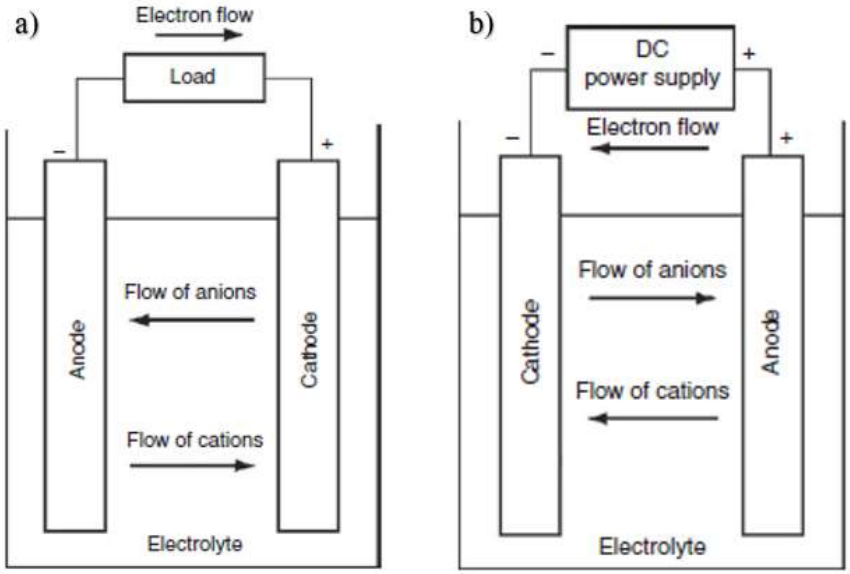

Figure 8 Electrochemical Operation of Battery Cell during a) Discharging b) Charging [9]

3.4.2. Voltage

The voltage of the LIB cell is determined by working voltage. This working voltage is the difference between chemical potential of the cathode (μ_C) and chemical potential of the anode (μ_A). The working voltage of LIB is also known as the open circuit voltage (OCV) and can be determined by the following formula;

$$E_{OCV} = \frac{\mu_A - \mu_C}{e}$$

Given that e is the value of electronic charge of the battery. The value of this working voltage is limited to certain boundaries as shown by Figure 9. The boundaries are separated into two factions, the highest occupied molecular orbital (HOMO) and lowest unoccupied molecular orbital (LUMO).

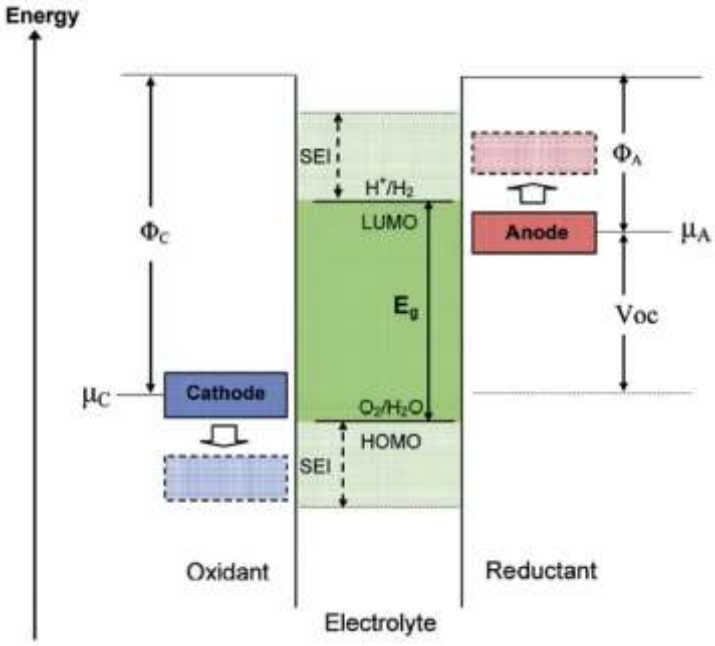

Figure 9 Relative Energy of the Electrolyte Window [27]

The selection of electrodes is essential in this case. The anode and cathode must have the value such that μ_A is below the LUMO and μ_C is higher than the HOMO line. If these requirements are not met, the electrolyte will be reduced on the anode or oxidised on the cathode and result in formation of SEI layer [28]. The formation of SEI layer will increase the internal resistance of the battery and results in the inability of electrolyte molecules to pass through to the active electrode surfaces. This is vital as it could prevent the reaction of the molecules with lithium ions and electrons. Additionally, increased degradation of the LIB performance in cycling is

observed as SEI layer thickens [13]. Further details on impact of SEI layer will be discussed in the degradation mechanism section (Section 3.5).

In real life application of LIB, internal impedance is a key factor that can cause voltage drop of LIB. Internal impedance is the total internal ionic resistance of the cell which includes all electrolyte, electrodes, current collector and active masses present [15]. Other major factors are the overpotential and polarization at both electrodes. The effect of all the mentioned factors on voltage drop is summarised by the formula below.

$$E = E_{OCV} - [(\eta_{ct})_a + (\eta_c)_a] - [(\eta_{ct})_c + (\eta_c)_c] - iR_i$$

Given that:

- E_{OCV} is electromotive force or open-circuit voltage of cell;
- $(\eta_{ct})_a$, $(\eta_{ct})_c$ are charge-transfer overvoltage at anode and cathode;
- $(\eta_c)_a$, $(\eta_c)_c$ are the concentration polarisation at anode and cathode;
- i is the operating current of the cell load; and
- R_i is the internal resistance of the cell.

Figure 10 shows how the cell voltage decreases as a function of current during discharge.

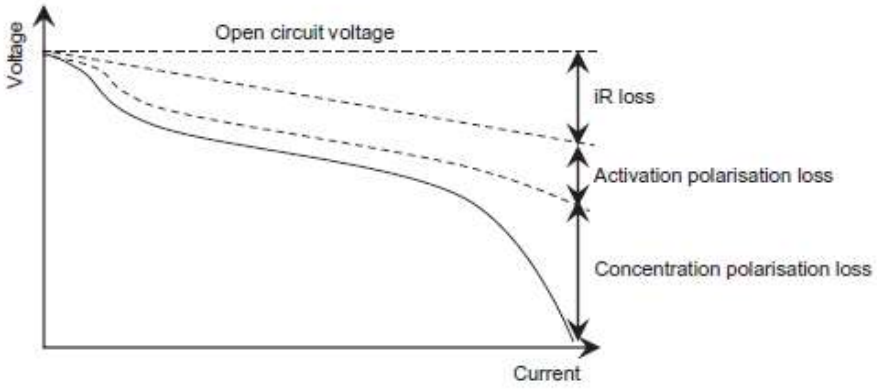

Figure 10 Cell Voltage as a Function of Current Used [9]

3.4.3. Battery Capacity, Energy & Coulombic Efficiency

Theoretically, the capacity of LIB is usually described as the amount of electric charge a cell can deliver under specific condition. For LIB, the capacity depends on the discharging current, temperature, cut-off voltage, and the amount and type of active materials used [29]. The variation of capacity by different discharge rates can be seen on Figure 11. Besides that, battery capacity is also expressed by the total sum of electricity present in the electrochemical reaction

occurring in the cell [15] and is usually defined in ampere-hour (Ah). Understanding the definition of capacity, it is noticed that a smaller cell will have lower capacity as it has a lower amount of active materials. However, the small cell size does not have an impact on the battery operating voltage [9]. Besides in ampere-hour, capacity can also be written as specific capacity (mAh/g or Ah/kg) which is derived from Faraday's law:

$$Q_{th} = \frac{nF}{M_w}$$

Given that, Q_{th} is the theoretical battery capacity, F is Faraday's constant, n is the number of electrons transferred from one electrode to another, and M_w is the molecular weight of the active material taking place in the electrochemical reaction.

The energy of the battery refers to how much work the battery can deliver until it reaches the cut off voltage, it is also considered as the highest value that a battery can deliver. In a charging and discharging curve (Figure 11), the total energy of battery corresponds to the area under the discharge curve [9]. The energy of LIB is usually defined in watthour and is calculated as the product of the battery capacity and the discharge voltage of the battery [29] as shown in the equation below.

$$Watthour(Wh) = voltage(V) \times amperehour(Ah)$$

In an ideal electrochemical cell, the cycling efficiency is specified as the Coulombic efficiency. Coulombic efficiency of a battery can be defined as the ratio between the total charge transferred during discharging (Q_{dis}) over the total charge transferred during charging (Q_{cha}) [9].

$$\eta_{coulombic} = \frac{Q_{dis}}{Q_{cha}}$$

According to Yang et al., 2018, the coulombic efficiency of a battery is directly correlated to the battery cycle life. High Coulombic efficiency indicated that the battery has a long cycle life. It is found that the coulombic efficiency is closely related to the degradation mechanism of LIB and can be utilised to predict the degradation rate of a battery [30].

3.4.4. Current Rates

Current rates or C-rates define the discharge rate of a battery and the current density which indicates the number of lithium ions that is moving between electrodes at a certain speed. At a higher C-rate, typically LIB capacity is lower, and the battery undergoes faster degradation. A rate of 1C means that LIB battery charge and discharge at a current which correspond to the

capacity of battery. If a battery has 0.1C rate, it means that the battery has a discharging time 10 times slower compared to a battery with 1C-rates [31].

Different C-rates will have impact on the LIB capacity during cycling. High C-rates will result in lower number of lithium ion available for the insertion to each electrode. It is because of high number of lithium ion transferred to the opposite electrodes, causing congestion for the lithium insertion [9]. At higher C-rates, slower lithium ions diffusion rate from electrolyte to electrode will cause a higher concentration gradient between them leading to overpotentials and encouraging battery degradation. In addition, if high C-rates is used during charging, it will be faster for the cell to reach the upper cut-off voltage. Consequently, lower LIB capacity will be obtained. On the other hand, high C-rates during discharge will cause the cell to reach lower cut-off voltage faster, resulting in capacity fade to be apparent [9]. As shown on Figure 11, higher value of C-rates will have faster capacity depletion. Additionally, high C-rates will cause strain in the electrodes, initiating crack of SEI and both active electrodes material [9].

In contrast with the high C-rates condition, lower C-rates provide stable and fast diffusion of lithium ions from the electrolytes to each electrode. This prevents the build-up of concentration gradient in the electrolyte [9]. With low C-rates, it is assumed that the capacity of LIB will be maintained. However, in real situation other factors such as temperature, number of operating cycle and type of electrodes used will also have impact on the battery capacity.

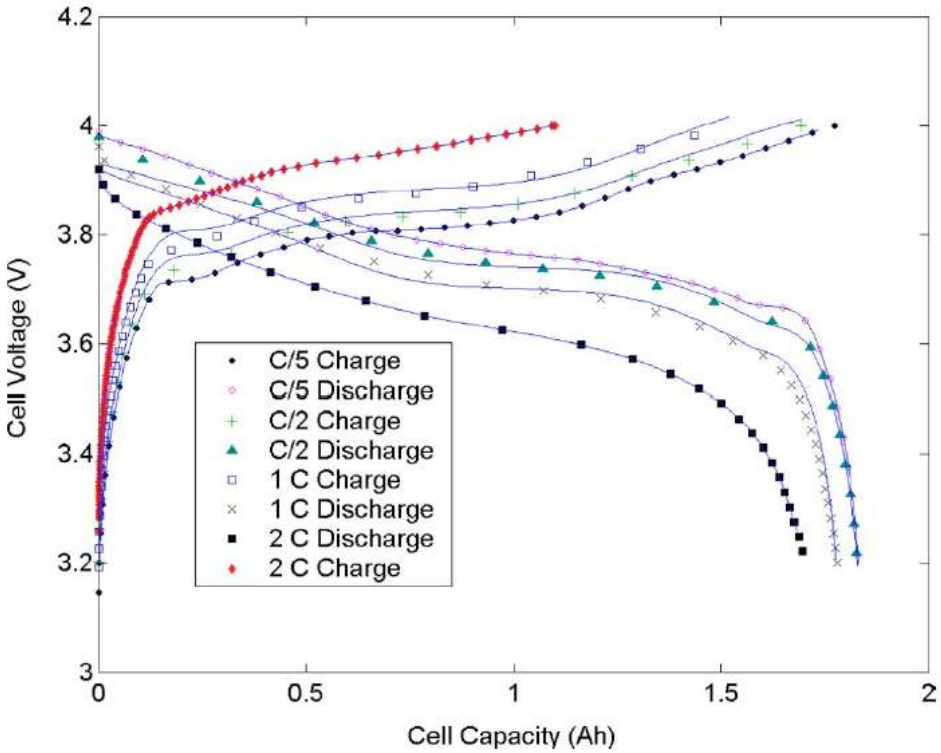

Figure 11 Charge and Discharge Curve Comparison for LIB [32]

3.4.5. Temperature

Operating temperature is also one of the main factors that could affect the performance of the battery. Similar to C-rates, high temperature will also speed up the degradation of LIB performance. However, unlike lower C-rates that are capable to maintain battery capacity, extremely low temperature will also increase the degradation of the battery. These operating temperatures are affected by both the internal and external condition of the battery. Therefore, both the condition of LIB and its surrounding are essential for the battery to perform optimally.

In a situation where LIB operates at high operating temperature, it is found that there will be more loss of active materials and lithium ions. Predominantly, higher temperature will create higher activation energy of the particles in LIB. This high activation energy introduces faster reaction inside the battery, including the unwanted chemical reaction [9]. At a certain point, the increased in temperature is desirable as it increase power capability and energy output. However, the long-term exposure of high temperature will result in the build-up of the unwanted reactions such as the formation and thickening of SEI layer. In short, high temperature is also able to accelerate the degradation mechanism of LIB. Moreover, the presence of high temperature in the LIB operating condition could trigger the de-orientation of both electrodes structure [9]. This phenomenon will change some of the active sites for lithium intercalation in the electrodes leading to less diffusion of lithium ions into the electrodes, decreasing battery capacity limit. Figure 12 shows how increasing temperature will have effect on the battery cycling capacity.

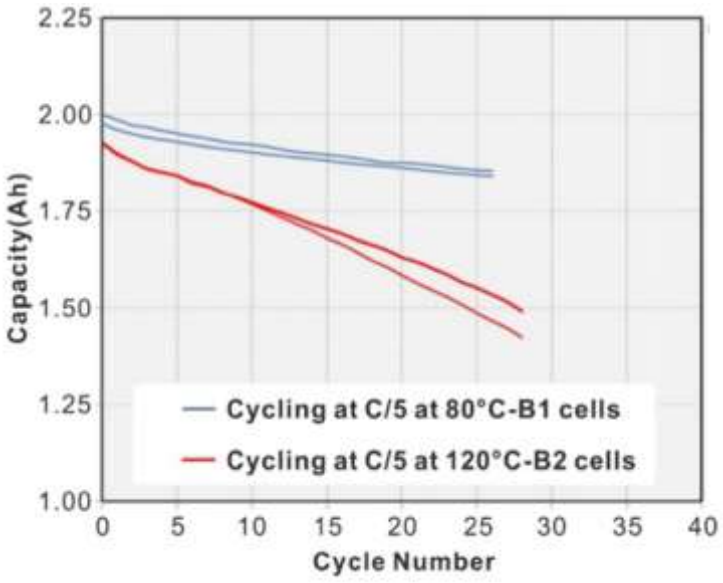

Figure 12 Effect of Temperature on LCO type LIB Cycling Capacity [33]

As previously stated, extremely low temperature is also the cause of an increase of LIB degradation. Using lower temperature, however, will result in the diffusion of lithium ions

becoming too slow, thus initiating lithium plating. The other disadvantage of low temperature is that it will affect the property of the battery electrolyte. By using lower temperature, the viscosity of the electrolyte will rise thus reducing the conductivity of lithium ions [33]. Therefore, it is preferable for the cell durability that the temperature is kept in the range of 25 – 35 °C, as it is found to be the optimal temperature range for most LIB.

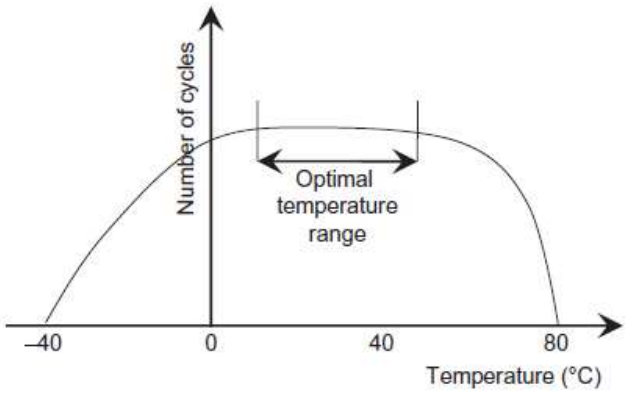

Figure 13 Illustration of the Optimal Temperature Range of LIB with Respect of Durability [9]

3.5. Major Degradation of LIB

Active degradation of LIB has become the major concern for many of its users in the world. Besides affecting the capacity of LIB, degradation of the battery also introduces safety issue of the LIB. There are 3 types of degradation mechanism: Loss of Lithium Inventory (LLI), Loss of Active Material of Negative Electrode (LAM_{NE}) and Loss of Active Material of Positive Electrode (LAM_{PE}) [34]. LLI is usually caused by the formation and decomposition of SEI layer, whereas LAM_{NE} and LAM_{PE} are usually the result of particle cracking and volume expansion of the electrodes. Figure 14 shows the different degradation mechanisms that could occur in LIB during cycling.

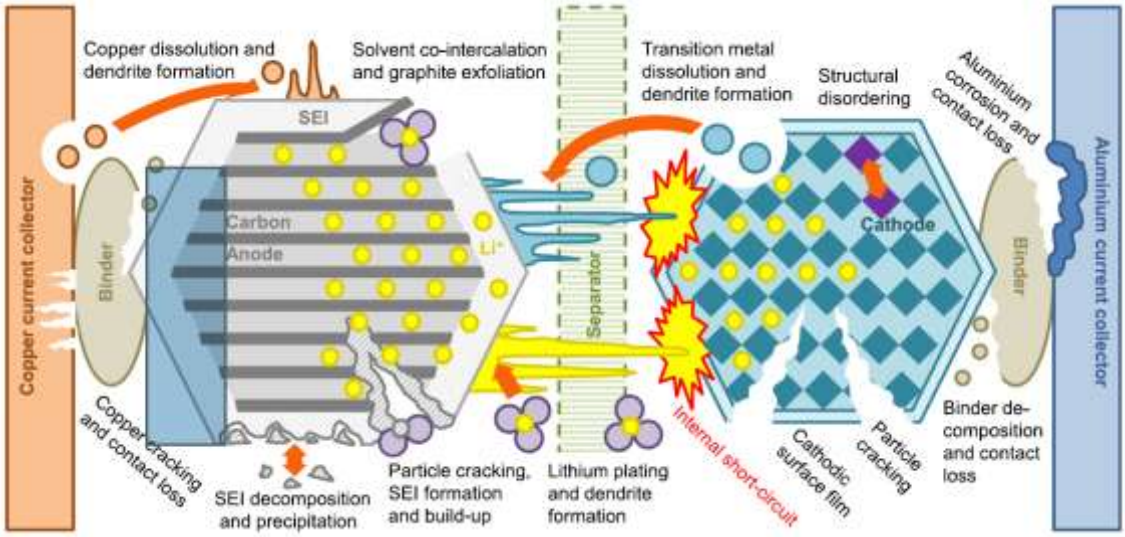

Figure 14 Degradation Mechanism in Li-ion cells [34]

The main degradation mechanisms are usually observed from decrease in battery capacity, increase of self-discharge rate and decrease in power. From all of the degradation mechanism shown in the figure, the major degradations of LIB during cycling are solid electrolyte interphase (SEI) formation and decomposition, volume expansion and particle cracking, and dendrite formation.

3.5.1. SEI Layer Formation and Decomposition

SEI layer formation is one example of LLI degradation mechanism of LIB. During lithium insertion into the graphene layer of the anode, μ_A falls above the LUMO energy. As previously stated, this results in the decomposition of electrolyte. The decomposed products will react to some lithium ions and electrons to form solid insoluble layer on the anode [24]. This layer is called the SEI layer. As generally known, lithium ions are carried by a solvation spheres in the electrolyte. Occasionally, during the intercalation of lithium ions, these solvation spheres are also intercalated in the graphene layer and leads to the de-structuring of the graphene layer. This phenomenon is also known as exfoliation [11]. In recent studies, a suitable choice of electrolyte is used such as ethylene carbonate (EC) or propylene carbonate (PC). This mixture of electrolyte enables the

formation of impermeable SEI layer which can avoid the co-intercalation process.

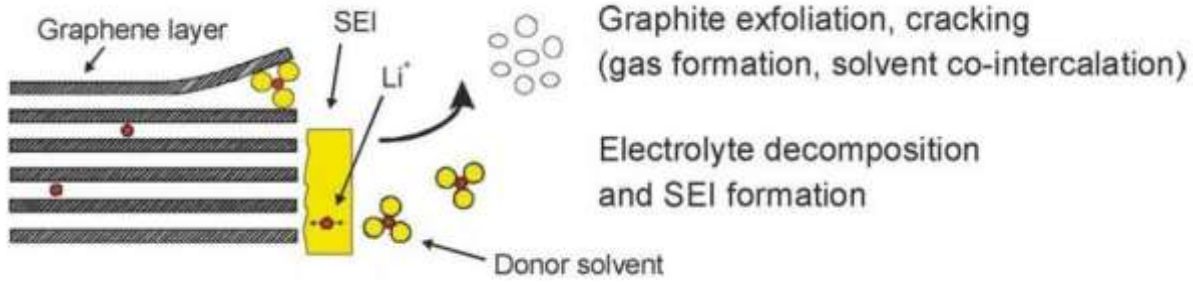

Figure 15 Graphene Exfoliation Process and SEI Layer Protective Function [11]

SEI layer has a possibility to thicken during each charge and discharge cycle. This is due to two things: electron exposure to electrolyte and some electrolyte molecule penetrating through to the anode surface. It is unfavourable when the SEI layer become thicker as it increases the internal resistance of the battery. Additionally, the continuous thickening of SEI layer consumes more lithium ions, thus decreasing the number of lithium ions available for the cycle. This could result in degrading of LIB capacity and coulombic efficiency [24]. Hence, researchers are currently developing the improved mixture of electrolyte to prevent this SEI growth.

Furthermore, the SEI layer has the probability to crack during cycling, leaving the active material surface exposed to the electrolytes. As a result, new formation of SEI layer will happen and more lithium ions will be consumed. This means there will be higher LLI and decreasing number of cyclable lithium, which leads to further decreasing in the capacity of the battery [9].

3.5.2. Volume Expansion and Particle Cracking

Volume expansion is one example of degradation mechanism of LIB which cause a change in bulk materials, especially in graphite. During the charging and discharging cycle, the graphite structure contract and expand due to the intercalation and deintercalation of lithium ions. This introduce mechanical stress to the carbon-carbon bond. The worst case is when cracking on the graphene layer can be observed [9]. Volume expansion can also cause cracking of the SEI layer initiate formation of new SEI layer. Thus, less lithium ions will be available for the battery cycle. This particle cracking could also occur on the cathode side and result in an increase of resistance. The effect of particle cracking might worsen by introducing the LIB to higher C-rates, resulting in higher LAM_{NE} and LAM_{PE}. Moreover, particle cracking mainly causes cathode to undergo structural change. These structural changes could have impact in de-orientation of lithium-ion active site, thus reducing the number of lithium ions that can diffused in. This phenomenon will adversely impact the battery's capacity fade and loss in electrochemical performance [9].

3.5.3. Dendrite Formation

Apart from SEI formation and particle cracking, the formation of dendrites and the growth of dendrites itself are also considered the critical degradation mechanism. These phenomena are amongst the obstacles that could prevent lithium ion battery to reach its highest capacity [35]. Lithium dendrite is a needle-like structure that is formed by the accumulation of lithium plated on the electrode surface. There are several factors that causes lithium dendrite formation, one of those factors being temperature. At low temperature, the kinetics of the cell will decrease and resulting to very slow diffusion of lithium ions to anode, slower than the electrical energy transferred. As a consequence, lithium ions will be plated to the polarised anode instead [9]. In the long run, the formation of lithium plate in electrode surface will induce the growth of spinel-structure dendrite. As shown in Figure 16, as the battery cycling continues, the lithium dendrites continue to grow. At some point, the lithium dendrite will start penetrating through the separator to reach the cathode, causing internal short circuit [36]. In the worst case, this short circuit might initiate internal thermal reaction or explosion.

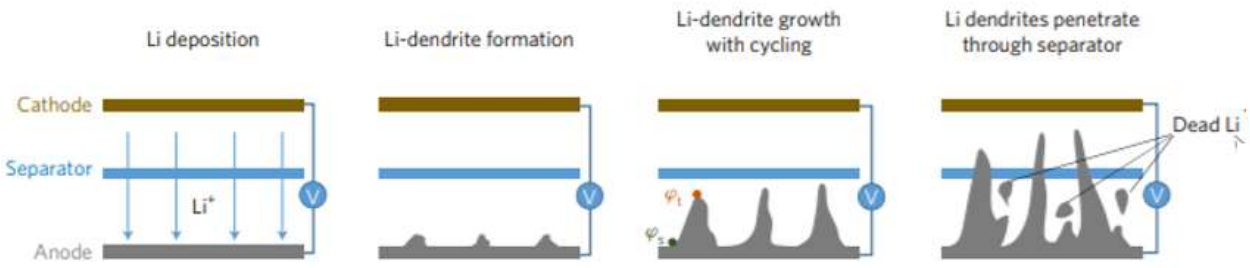

Figure 16 Dendrite Growth in LIB [36]

The process of dendrite formation consumes cyclable lithium ions, decreasing the battery capacity. Unlike the formation SEI layer, lithium plating is a reversible process as lithium dendrite can be oxidised again into cyclable lithium ions. However, this will cause overpotential which unfavourable for battery operating condition [9].

4. Data Collection and Analysis

The following section presents the data collected in order to understand the effect of different condition on battery performance. This section will focus on the NMC and LFP battery data when exposed to different operating temperature and C-rates. The full data of degradation can be looked up on Appendix A.

4.1. Effect of C-Rates on Initial Capacity of NMC and LFP

As previously discussed, the value of C-rates used for battery operation determines the initial capacity of a battery. This section will prove the theory on how different C-rates affect a battery's initial capacity.

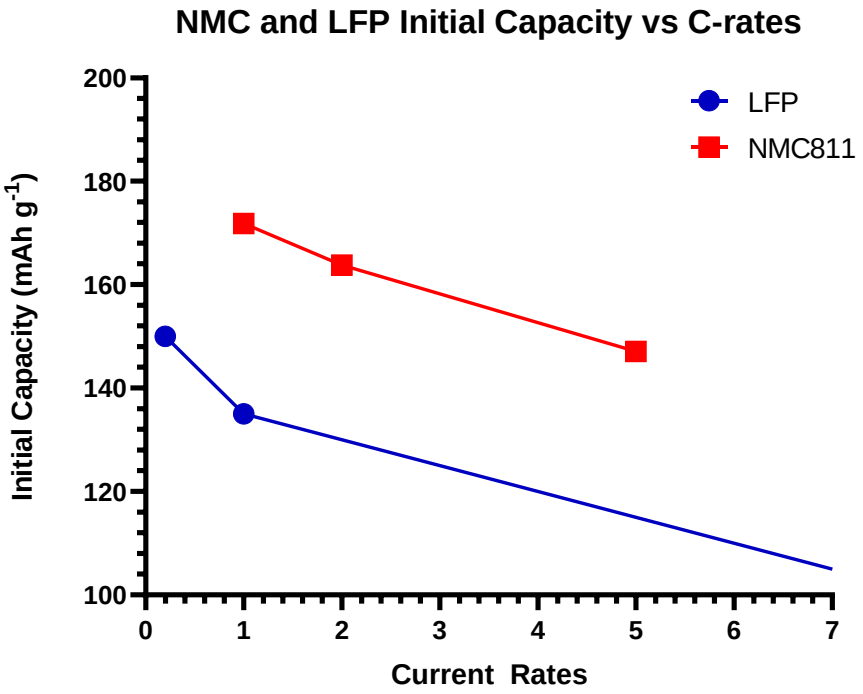

Figure 17 Effect of C-Rates on NMC and LFP Initial Capacity

Figure 17 shows that the initial capacity of NMC and LFP decreases as the C-rate increases. Higher C-rates will cause the battery to reach the cut-off voltage faster and a lower battery capacity will be obtained. This is clearly illustrated by Figure 11 where battery with higher C-rates will stop charging at lower capacity.

In addition, Figure 17 also emphasize on the different initial capacities of NMC and LFP. The graph reveals that NMC has an initial capacity of 171.8 mAh g^{-1} which is higher than LFP 's initial capacity of 135 mAh g^{-1} when operated at 1C. The superior battery capacity of NMC to LFP can be explained by the structure of the NMC itself. The battery that is used in the graph

is NMC811 where the battery has much higher nickel content compared to cobalt and manganese. As discussed in section 3.2.1, the composition of Ni in NMC contributes to the battery capacity. Higher Ni content will result in higher capacity, but with the price of the battery safety as there will be more Ni^{4+} formed during charging.

4.2. Effect of C-Rates on Capacity Degradation of NMC and LFP

Apart from affecting initial capacity of LIB, different C-rates used also affect the capacity degradation of the battery during cycling operation. The following graphs shows the effect of changing C-rates on percentage capacity degradation over a cycle.

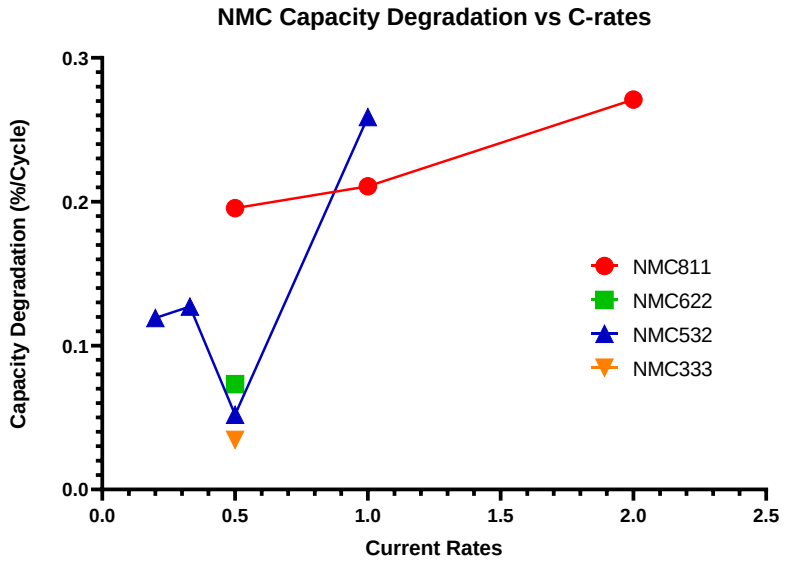

Figure 18 Effect of C-Rates on NMC's Capacity Degradation

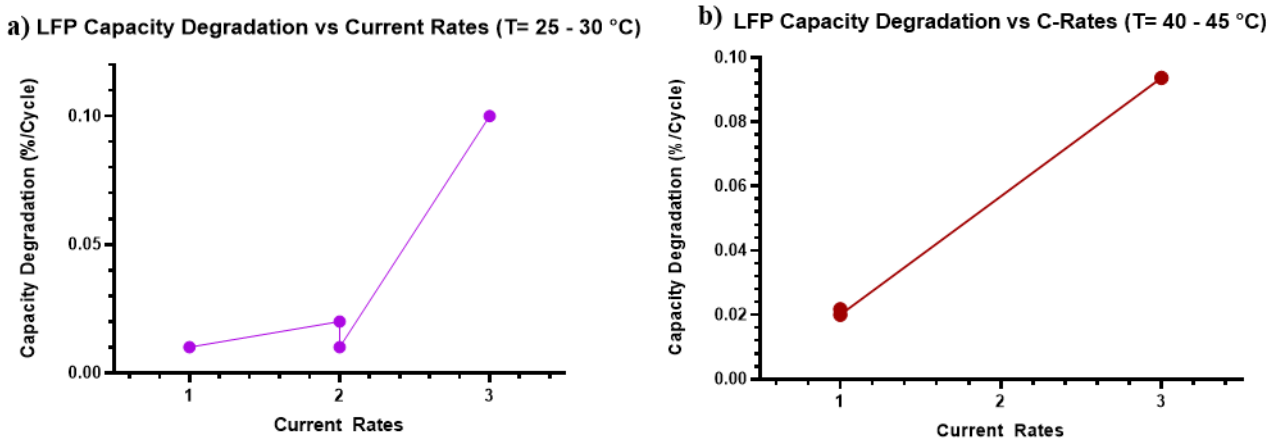

Figure 19 Effect of C-Rates on LFP's Capacity Degradation at a) T= 25 - 30 °C b) T= 40 - 45 °C

Generally, Figure 18 and Figure 19 highlight how increasing C-rates increases the capacity fade of LIB. As reviewed in section 3.4.4, increasing the C-rates makes diffusion of lithium during intercalation process relatively slower than the movement of lithium ions through the separator and results in congestion for lithium insertion. A large number of lithium ions near the electrode surface could will also result in a high concentration gradient to develop near the electrode surface and lead to overpotential. These overpotential then initiate the decomposition of electrolyte, thus, starting the formation of SEI on the electrode surface. From Section 3.5.1, it is known that the formation of SEI is one of the reasons of loss of cyclable lithium ions. More loss of cyclable lithium-ions means that the battery will have lower capacity with each passing time. Aside from that, high C-rates could also lead to cracking of SEI layer, which initiate the formation of SEI layer which consume more lithium ions. On the other hand, lower C-rate give more time for diffusion of lithium during intercalation, preventing concentration gradient to build up, thus maintaining the capacity of LIB.

Figure 18 illustrates how different values of C-rates will affect the degradation of NMC. NMC811 has an increase of 38.6% in its capacity degradation as C-rate is increased from 0.5C to 2C. Moreover, NMC811 has the highest capacity degradation compared to other types of NMC (0.27%/cycle at 2C). It is because the high composition of nickel in the structure of NMC cathode. Larger value of nickel will lead to higher number of unstable tetravalent nickel to be formed, resulting in more unwanted reactions to occur. Aside from high nickel composition, the high degradation of NMC811 is also caused by low ratio of manganese and cobalt as it gives low safety characteristic or low stability of the battery. The low stability affects the battery by lowering the battery's resistance to degradation, thus higher degradation occurs.

Moreover, Figure 19 shows how the C-rates affects the degradation of LFP battery. The graph shows the exact same trend with the previous graph. LFP shows an increase in the rate of capacity degradation about 900% when subjected to a temperature range between 25 - 30 °C with an increase of C-rate from 1C to 3C. However, compared to NMC, LFP has much lower capacity degradation (0.02%/cycle at 2C). This is caused by the high stability of olivine LFP structure. As explained in Section 3.2.2, the small structural change of LFP during intercalation and de-intercalation results in high resistance of the battery to degradation. Therefore, LFP shows lower degradation compared to NMC due to their difference in stability.

4.3. Effect of Temperature on Capacity Degradation of NMC and LFP

Aside from C-rates, temperature is also a critical factor of LIB's capacity fade. The below graphs show how temperature could affect the cycling capacity degradation of NMC and LFP.

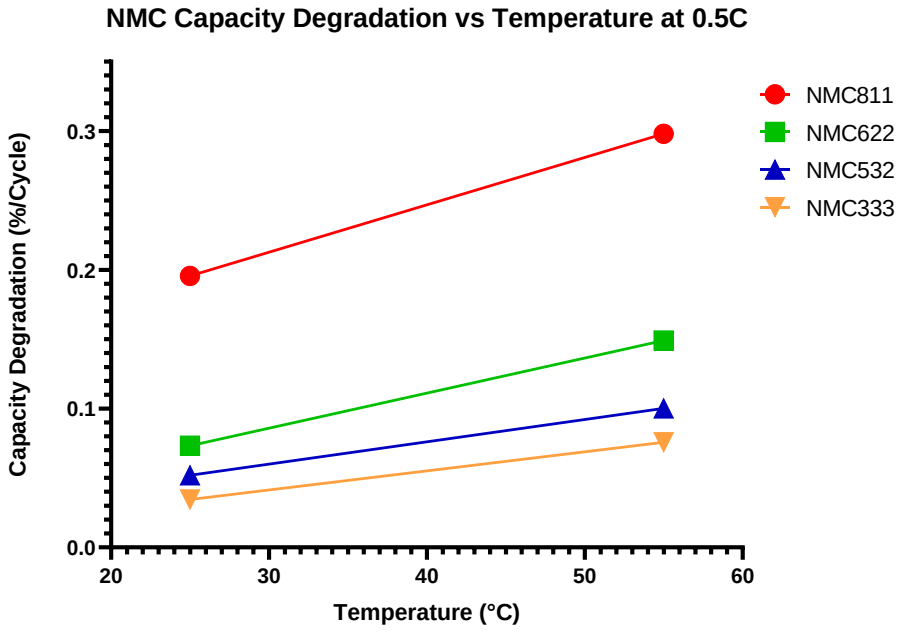

Figure 20 Effect of Temperature on NMC's Capacity Degradation at 0.5C

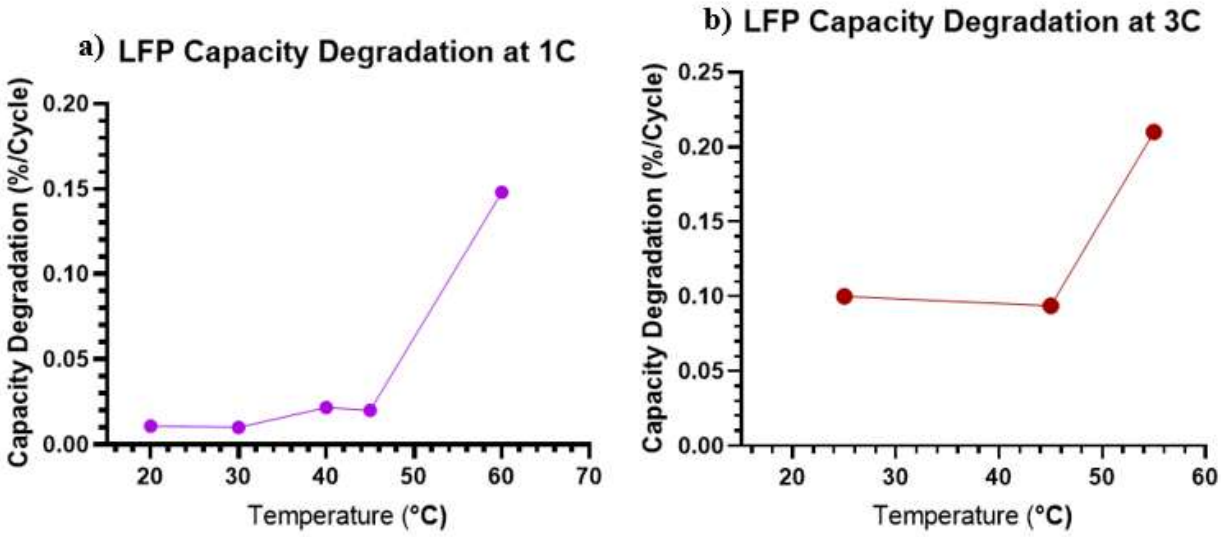

Figure 21 Effect of Temperature on NMC's Capacity Degradation at a) 1C b) 3C

Figure 20 and Figure 21 establish the theory that higher temperature will cause higher degradation of the battery capacity. In general, at high temperature, there will be faster reaction occurring in the battery. One such reaction is that the formation of SEI layer that definitely induce the capacity fade. Besides that, the increase of temperature also speeds up the wearing down of SEI layer, thus more lithium ions are consumed to repair the protective layer. Higher loss of cyclable lithium-ions means lower cycling capacity of the battery. Even though no data exists for degradation at extremely low temperature, it can be expected from the known trends that there will be increase of degradation. This is behind the reason that at low temperature, there will be less activation energy, making the diffusion of lithium ion slower compared to electrical energy transferred. As a result, rather than being diffused into the graphene layers, lithium is plated on the electrode surface instead, increasing the resistance of the cell [9]. The phenomenon can also be considered as LLI and lowers the cycling capacity of LIB.

Figure 20 shows how increasing the temperature will have an increase in degradation of NMC. From the graph, NMC capacity degradation rate is seen to have an average increase about 92% as the operating temperature is increased from 25 °C to 55 °C. The graph clearly illustrates that NMC811 still has the highest capacity degradation rate among other types of NMC (about 0.2%/cycle at T = 25 °C and 0.3%/cycle at T = 55 °C). This is an additional proof that increasing the composition of nickel and lowering the composition of manganese and cobalt in NMC structure will cause decay in the LIB stability, reducing its resistance to performance degradation.

Subsequently, Figure 21 follows the same trend as Figure 20 and shows that the increase of LFP operating temperature will increase the rate of degradation of the battery. From Figure 21a, LFP degradation rate has an increase of about 1263% when the operating temperature of the battery is raised from 20 °C to 60 °C. Despite the significant increase of LFP degradation rate, Figure 16a) shows that at 60 °C, LFP has a capacity degradation rate of 0.148%/cycle. Therefore, even at high temperature of 60 °C, the capacity degradation of LFP is still lower than the capacity degradation of NMC at 55 °C.

5. Discussion

From the observation of Figure 17, NMC has higher initial battery capacity compared to LFP battery. As elucidated on this report, the reason behind the high capacity of NMC is the composition of nickel in the NMC structure. Furthermore, in condition where the C-rates used are raised, the initial battery capacity of both LFP and NMC will decrease due to limitation of LIB battery capacity reach. Moreover, despite the high capacity of NMC, when high C-rates is utilised in the operation, NMC will show a higher degradation when compared to LFP. As explained in the previous section, the stability of the battery is directly related to LIB degradation. In this case, the olivine structure of LFP results in superior stability compared to NMC. If we look at the data that have been gathered, change in temperature has higher increase in degradation rate of LIB capacity. Thus, assuming only C-rates and temperature are varied, effect of change in temperature will be more dominant compared to change in C-rates.

Taking a look at the previous section, the degradation mechanism of NMC and LFP is significantly affected by different values of C-rates and Temperature. The two parameters have a similar regarding LIB degradation. For high C-rates, the increase in degradation is mostly in consequence of the local overpotential in the electrolyte which leads to various effects. One example is that the initiation of SEI layer and the thickening of the layer, specifically the increasing consumption of cyclable lithium ions.

In reference of Section 3.5, the loss of cyclable lithium ions will bring about the degradation of the LIB capacity. On the other hand, it is proven that the use of lower C-rates is capable to maintain the LIB battery capacity. It is realised that the high operating temperature is also related to the increasing formation of SEI layer. However, the high temperature itself also impacts the de-orientation of negative and positive electrodes, as well as SEI layer which also induce the degradation of LIB.

The changing structure of electrodes will consequently change some active sites for lithium ion to diffuse in, limiting the number of occurring intercalations. Besides that, high temperature also introduce wear and initiate the breakdown of SEI layer. This result in SEI layer requiring repairs and more consumption of lithium ions. Extremely low temperature is also a factor that could speed up battery degradation. By having extremely low temperatures, lithium plating can occur. Therefore, both temperature and C-rates are essential for optimal LIB performance.

Due to the high stability of LFP, it is expected that this type of battery is suitable to be used for frequency regulation storage as the system usually utilises high C-rates to operate. On the other hand, NMC that has lower stability than LFP are preferably to be used as stationary energy storage, where low C-rate is used. This is also backed by the high capacity of NMC, especially NMC811. In Australia, where the mean temperature is 30 °C, NMC and LFP are expected to be performing optimally.

The predicted performance of NMC811, NMC333, and LFP can be predicted by the formula below.

$$Final\ Capacity = Initial\ Capacity\ \times (Number\ of\ Cycles \times Degradation\ Rate)$$

Assuming that all three batteries are performing in the same condition, the number of cycles for the batteries to run-out (final capacity equals to zero) can be calculated.

Table 1 Data of Calculation for Number of Cycles to Reach Runout for LFP, NMC333, and NMC811

Battery	Initial Capacity (mAh g^{-1})	Final Capacity (mAh g^{-1})	Degradation Rate (%/cycle)	Number of Cycles
LFP	135	0	0.0053	18906
NMC333	171.8	0	0.21	475
NMC811	171	0	0.09	1111

As shown by the calculation result, LFP has the highest cycle before reaching runout. Therefore, LFP is more suitable to be used for a high-cycling system in Australia.

6. Conclusion and Recommendation

Both NMC and LFP have a superior capacity and cycling stability compared to other cathode materials for LIB. However, they have distinct benefits and drawbacks. This thesis project examines how these differences of NMC and LFP could affect their use for various grid usage. The outcomes of this project are briefly explained below:

a) Operating C-rates of LIB have dramatic impact on the initial capacity of NMC and LFP. The increase of C-rates will decrease the initial capacity of both types of LIB.
b) In condition where higher C-rate is used for battery operation, LIB will have higher degradation rate. Similarly, higher operating temperature will also result in higher degradation rate of the battery.
c) Among all degradation mechanisms, SEI formation, dendrite formation, and particle cracking are the major degradation mechanisms. However, SEI formation is the most critical as the process is closely related to the two factors of LIB degradation which are temperature and C-rates.
d) For usage in grid, NMC is more suitable to be used in stationary energy storage system where high energy stored is the system primary concern.
e) On the other hand, LFP is more suitable to be used in frequency regulation as LFP has excellent stability to withstand higher C-rates.
f) Between LFP, NMC811, and NMC333, LFP shows the best ability to be used in high cycling system, despite providing a lower capacity compared to NMC811 and NMC333.

For improvement of this project, the following recommendations are provided in consideration of eliminating the limitations of this thesis in the future.

a) This report only assume that other parameters are the same for every battery and only considers the effect of temperature and C-rates of LIB degradation. It is important to explore the effect of different battery condition used, such as type of electrolyte used and the type of anode used, as well as the battery operating voltage.
b) Explore different degradation mechanism of LIBs to understand more about what factor is affecting the performance of the battery.
c) Further research on various use of grids, including their operating mechanisms are required to understand the necessary qualification needed for choosing the suitable type of LIB needed to be used for the system.

References

[1] I. Dincer, Comprehensive Energy System, 1st ed., Amsterdam: Elsevier Inc., 2018.

[2] C. Julien, A. Mauger, A. Vijh and K. Zaghib, Lithium Batteries: Science and Technology, New York: Springer International Publishing, 2016.

[3] H. C. Hesse, M. Schimpe, D. Kucevic and A. Jossen, "Lithium-Ion Battery Storage for the Grid—A Review of Stationary Battery Storage System Design Tailored for Applications in Modern Power Grids," *Energies,* vol. 10, 2017.

[4] CSIRO, Bureau of Meteorology, "Australia's Changing Climate," Asutralia Government Bureau of Meteorology, Canberra, 2016.

[5] C. R. Birkl, M. R. Roberts, E. McTurk, P. G. Bruce and D. A. Howey, "Degradation diagnostics for lithium ion cells," *Journal of Power Sources,* pp. 373-386, 2017.

[6] E. O. Ogunniyi and H. Pienaar, "Overview of Battery Energy Storage System Advancement for Renewable (Photovoltaic) Energy Applications," 2017.

[7] I. Atteya, N. Fahmi, D. Strickland and H. Ashour, "Utilization of Battery Energy Storage System (BESS) in Smart Grid : A Review," *Renewable Energy and Power Quality Journal,* vol. 1, no. 14, 2016.

[8] J. Kang, F. Yan, P. Zhang and C. Du, "Comparison of comprehensive properties of Ni-MH (nickel-metal hydride) and Li-ion (lithium-ion) batteries in terms of energy efficiency," *Journal of Power Sources,* vol. 70, pp. 618-625, 2014.

[9] M. S. Islam and C. A. J. Fisher, "Lithium and sodium battery cathode materials: computational insights into voltage, diffusion and nanostructural properties," *Chem. Soc. Rev.,* pp. 43,185, 2014.

[10] H. Berg, Batteries for Electric Vehicles Materials and Electrochemistry, Cambridge: Cambridge University Press, 2015.

[11] D. Deng, "Li-ion batteries: basics, progress, and challenges," Society of Chemical Industry and John Wiley & Sons Ltd., 2015.

[12] L. Monconduit, L. Croguennec and R. Dedryvère, Electrodes for Li-ion Batteries: Materials, Mechanisms and Performance, Somerset: Wiley, 2015.

[13] V. Deimede and C. Elmasides, "Separators for Lithium-Ion Batteries: A Review on the Production Processes and Recent Developments," *Energy Technology,* vol. 3, pp. 453-468, 2015.

[14] M. B. Pinson and M. Z. Bazani, "Theory of SEI Formation in Rechargable Batteries: Capacity Fade, Accelerated Aging and Lifetime Prediction," *Journal of The Electrochemistry Society,* p. 160, 2013.

[15] R. Wagner, N. Preschitschek, S. Passerini, J. Leker and M. Winter, "Current research trends and prospects among the various materials and designs used in lithium-based batteries," *Journal of Applied Electrochemistry,* vol. 43, pp. 481-496, 2013.

[16] D. Linden and T. B. Reddy, Linden's Handbook of Batteries, 4th ed., McGraw-Hill Professional Publishing, 2010.

[17] S.-M. Bak, E. Hu, Y. Zhou, X. Yu, S. D. Senanayake, S.-J. Cho, K.-B. Kim, K. Y. Chung, X.-Q. Yang and K.-W. Nam, "Structural CHanges and Thermal Stability of Charged $LiNi_xMn_yCo_zO_2$ Cathode Materials Studied by COmbined In Situ Time-Resolved XRD and Mass Spectroscopy," *Applied Materials a& Interfaces,* vol. 6, pp. 22594-22601, 2014.

[18] M. M. Doeff, "Battery Cathodes," in *Batteries for Sustainability: Selected Entries from the Encyclopedia of Sustainability Science and Technology*, R. A. Meyers, Ed., Berkeley, Lawrence Berkeley National Laboratory, 2013.

[19] S. Ma, M. Jiang, P. Tao, C. Song, J. Wu, J. Wang and T. Deng, "Temperature Effect and Thermal Impact in Lithium-Ion Batteries: A Review," *Progress in Natural Science: Materials International,* vol. 28, pp. 653-666, 2018.

[20] L. Ma, M. Nie, J. Xia and J. R. Dahn, "A systematic study on the reactivity of different grades of charged $Li[Ni_xMn_yCo_z]O_2$ with electrolyte at elevated

temperatures using accelerating rate calorimetry," *Journal of Power Sources,* vol. 327, pp. 145-150, 2016.

[21] R. Genieser, S. Ferrari, M. Loveridge, S. Beattie, R. Beanland, H. Amari, G. West and R. Bhagat, "Lithium ion batteries (NMC/graphite) cycling at 80 °C: Different electrolytes and related degradation mechanism," *Journal of Power Sources,* vol. 373, pp. 172-183, 2018.

[22] A. K. Padhi, K. S. Nanjundaswamy and J. B. Goodenough, "Phospho-olivines as Positive-Electrode Materials for Rechargeable Lithium Batteries," *Journal of the Electrochemical Society,* vol. 144, 1997.

[23] B. Wu, Y. Ren and N. Li, "$LiFePO_4$ Cathode Material," in *Electric Vehicles â€“ The Benefits and Barriers, Dr. Seref Soylu (Ed.),* Beijing, InTech, 2011, pp. 199-216.

[24] V. Sharova, A. Moretti, T. Diemant, A. Varzi, R. J. Behma and S. Passerinia, "Comparative study of imide-based Li salts as electrolyte additives for Li-ion batteries," *Journal of Power Sources,* vol. 375, pp. 43-52, 2018.

[25] S. Goriparti, E. Miele, F. D. Angelis, E. D. Fabrizio, R. P. Zaccaria and C. Capiglia, "Review on recent progress of nanostructured anode materials for Li-ion batteries," *Journal of Power Sources,* vol. 257, pp. 421-443, 2014.

[26] S. J. An, J. Li, C. Daniel, D. Mohanty and S. Nagpure, "The state of understanding of the lithium-ion-battery graphite solid electrolyte interphase (SEI) and its relationship to formation cycling," *Journal of Power Sources,* vol. 105, pp. 52-76, 2016.

[27] L. Ji, Z. Lin, M. Alcoutlabi and X. Zhang, "Recent developments in nanostructured anode materials for rechargeable lithium-ion batteries," *Energy & Environmental Science,* vol. 4, p. 2682, 2011.

[28] S. Chauque, F. Oliva, A. Visintin, D. Barraco, E. P. M. Leiva and O. R. Cámara, "Lithium titanate as anode material for lithium ion batteries: Synthesis, post-treatment and its electrochemical response," *Journal of Power Sources,* vol. 799, pp. 142-155, 2017.

[29] A. Wang, S. Kadam, H. Li, S. Shi and Y. Qi, "Review on modeling of the anode solid electrolyte interphase (SEI) for lithium-ion batteries," *nature partner journals*, vol. 15, 2018.

[30] C. Liu, Z. G. Neale and G. Cao, "Understanding electrochemical potentials of cathode materials in rechargeable batteries," *Materials Today*, vol. 19, 2016.

[31] R. Korthauer, Lithium_ion Batteries: Basics and Applications, Berlin: Springer-Verlag GmbH Germany, 2018.

[32] F. Yang, D. Wang, Y. Zhao, K.-L. Tsui and S. J. Bae, "A Study of the Relationship Between Coulombic Efficiency and Capacity Degradation of Commercial Lithium-Ion Batteries," *Energy*, vol. 145, pp. 486-495, 2018.

[33] A. Perez, V. Quintero, F. Jaramillo, H. Rozas, D. Jimenez, M. Orchard and R. Moreno, "Characterization of the degradation process of lithium-ion batteries when discharged at different current rates," *SYSTEMS AND CONTROL ENGINEERING*, vol. 232, pp. 1075-1089, 2018.

[34] S. Santhanagopalan, Q. Guo and R. E. White, "Parameter Estimation and Model Discrimination for a Lithium-Ion Cell," *Journal of The Electrochemical Society*, vol. 154, pp. A198-A206, 2017.

[35] G. Rong, X. Zhang, W. Zhao, Y. Qiu, M. Liu, F. Ye, Y. Xu, J. Chen, Y. Hou, W. Li, W. Duan and Y. Zhang, "Liquid-Phase electrochemical Scanning Electron Microscopy for In SItu Investigation of Lithium dendrite Growth and Dissolution," *Advance Materials*, vol. 29, 2017.

[36] Y. Liu, Q. Liu, L. Xin, Y. Liu, F. Yang, E. A. Stach and J. Xie, "Making Li-Metal Electrodes Rechargable by Controlling the Dendrite Growth Direction," *Natural Energy*, vol. 2, 2017.

[37] Y. Zhang, C.-Y. Wang and X. Tang, "Cycling Degradation of Automotive LiFePO4 Lithium-Ion Battery," *Journal of Power Sources*, vol. 196, pp. 1513-1520, 2011.

[38] M. Safari and C. Delacourt, "Aging of a Commercial Graphite/$LiFePO_4$ Cell," *Journal of The Electrochemical Society*, vol. 158, pp. A1123-A1135, 2011.

[39] Y. Zheng, Y.-B. He, K. Qian, B. Li, X. Wang, J. Li, C. Miao and F. Kang, "Effects of State of Charge on the Degradation of $LiFePO_4$/Graphite Batteries during Accelerated Storage Test," *Journal of Alloys and Compounds,* vol. 639, pp. 406-414, 2015.

[40] D. Li, D. L. Danilov, J. Xie, L. Rajimakers, L. Gao and Y. Yang, "Degradation Mechanism of C6/$LiFePO_4$ Batteries: Experimental Analyses of Calendar Aging," *Electrochimica Acta,* vol. 190, pp. 1124-1133, 2016.

[41] J.-F. Li, Y.-S. Lin, C.-H. Lin and K.-C. Chen, "Three-Parameter Modeling of Nonlinear Capacity Fade for Lithium-Ion Batteries at Various Cycling Conditions," *Journal of The Electrochemical Society,* vol. 164, no. 12, pp. A2767-A2776, 2017.

[42] M. Shimomura, T. Mochizuki and M. Takano, "Numerical Analysis of High-Performance Lithium-Ion and Lead-Acid Batteries with Capacity Fade for an Off-Grid Residential PV System," *Journal of Energy Engineering,* vol. 142, no. 1, 2016.

[43] C.-C. Yang, J.-H. Jang and J.-R. Jiang, "Preparation of Carbon and Oxide Co-modified $LiFePO_4$ Cathode Material for High Performance Lithium-Ion Battery," *Material Chemistry and Physiscs,* vol. 165, pp. 196-206, 2015.

[44] K. Jalkanen, J. Karppinen, L. Skogström, T. Laurila, M. Nisula and K. Vuorilehto, "Cycle aging of commercial NMC/graphite pouch cells at different temperatures," *Applied Energy,* vol. 154, pp. 160-172, 2015.

[45] R. Genieser, S. Ferrari, M. Loveridge, S. D. Beattie, R. Beanland, H. Amari, G. West and R. Bhagat, "Lithium ion batteries (NMC/graphite) cycling at 80 °C: Different electrolytes and related degradation mechanism," *Journal of Power Sources,* vol. 373, pp. 172-183, 2018.

[46] J. Wang, J. Purewal, P. Liu, J. Hicks-Garner, S. Soukazian, E. Sherman, A. Sorenson, L. Vu, H. Tataria and M. W. Verbrugge, "Degradation of lithium ion batteries employing graphite negatives and nickelecobaltemanganese oxide þ spinel manganese oxide positives: Part 1, aging mechanisms and life estimation," *Journal of Power Sources,* vol. 269, pp. 937-948, 2014.

[47] N. Yabuuchi and T. Ohzuku, "Electrochemical behaviors of $LiCo_{1/3}Ni_{1/}3Mn_{1/3}O_2$ in lithium batteries at elevated temperatures," *Journal of Power Sources,* vol. 146, pp. 636-639, 2005.

[48] Y. Leng, S. Ge, D. Marple, X.-G. Yang, C. Bauer, P. Lamp and C.-Y. Wang, "Electrochemical Cycle-Life Characterization of High Energy Lithium-Ion Cells with Thick Li(Ni0.6Mn0.2Co0.2)O2 and Graphite Electrodes," *Journal of The Electrochemical Society,* vol. 164, no. 6, pp. A1037-A1049, 2017.

[49] X. Zhao, Q.-C. Zhuang, C. Wu, K. Wu, J.-M. Xu, M.-Y. Zhang and X.-L. Sun, "Impedance Studies on the Capacity Fading Mechanism of $Li(Ni_{0.5}Co_{0.2}Mn_{0.3})O_2$ Cathode with High-Voltage and High-Temperature," *Journal of The Electrochemical Society,* vol. 162, no. 14, pp. A2770-A2779, 2015.

[50] S. Chang, Y. Chen, Y. Li, J. Guo, Q. Su, J. Zhu, G. Cao and W. Li, "Improvement of the high-voltage electrochemical properties of Li $[Ni_{0.5}Co_{0.2}Mn_{0.3}]O_2$@ ZrO_2 cathode materials with liquid phase modification," *Journal of Alloys and Compounds,* vol. 781, pp. 496-503, 2019.

[51] Y. Lei, J. Ai, S. Yang, C. Lai and Q. Xu, "Nb-doping in $LiNi_{0.8}Co_{0.1}Mn_{0.1}O_2$ cathode material: Effect on the cycling stability and voltage decay at high rates," *Journal of the Taiwan Institute of Chemical Engineers,* vol. 97, pp. 255-263, 2019.

[52] J. W. Kim, J. J. Travis, E. Hu, K.-W. Nam, S. C. Kim, C. S. Kang, J.-H. Woo, X.-Q. Yang, S. M. George, K. H. Oh, S.-J. Cho and S.-H. Lee, "Unexpected high power performance of atomic layer deposition coated Li[Ni1/3Mn1/3Co1/3]O2 cathodes," *Journal of Power Sources,* vol. 254, pp. 190-197, 2014.

[53] B. Stiaszny, J. C. Ziegler, E. E. Krauß, J. P. Schmidt and E. Ivers-Tiffée, "Electrochemical characterization and post-mortem analysis of aged LiMn2O4eLi(Ni0.5Mn0.3Co0.2)O2/graphite lithium ion batteries. Part I: Cycle aging," *Journal of Power Sources,* vol. 251, pp. 439-450, 2014.

[54] H.-J. Noh, S. Youn, C. S. Yoon and Y.-K. Sun, "Comparison of the structural and electrochemical properties of layered $Li[Ni_xCo_yMn_z]O_2$ (x = 1/4, 1/3, 0.5, 0.6, 0.7, 0.8 and 0.85) cathode material for lithium-ion batteries," *Journal of Power Soures,* vol. 233, pp. 121-130, 2013.

[55] S. S. Choi and H. S. Lim, "Factors that affect cycle-life and possible degradation mechanisms of a Li-ion cell based on $LiCoO_2$," *Journal of Power Sources,* vol. 111, pp. 130-136, 2002.

[56] X.-L. Wang, K. An, L. Cai, Z. Feng, S. E. Nagler, C. Daniel, K. J. Rhodes, A. D. Stoica, H. D. Skorpenske, C. Liang, W. Zhang, J. Kim, Y. Qi and S. J. Harris, "Visualizing the chemistry and structure dynamics in lithium-ion batteries by in-situ neutron diffraction," *Sci.Rep,* 2012.

Appendix A: Degradation Data of NMC and LFP

Table 2 Degradation Data of NMC and LFP

No.	Cathode	Anode	Electrolyte	C-Rate	T (°C)	Initial Capacity (Ah)	Final Capacity (Ah)	Capacity Fade (%)	Cycle	Degradation		Degradation Mechanism	References
										10^-3 Ah/Cycle	%/Cycle		
1	$LiFePO_4$ (LFP)	Graphite	LiClO4 in EC-DME	3	45	1.6	0.7	56.25	600	1.50	0.09	Loss of cyclable lithium due to SEI layer growth	[37]
2	$LiFePO_4$ (LFP)	Graphite	LiClO4 in EC-DME	3	-10	16.4	9.8	40.24	600	11.00	0.07	Loss of cyclable lithium due to SEI layer growth	[37]
3	$LiFePO_4$ (LFP)	Graphite	LiPF6 in EC-DME	1	25	2.3	1.8	21.74	4110	0.12	0.01	Loss of cyclable lithium	[38]
4	$LiFePO_4$ (LFP)	Graphite	LiPF6 in EC-DME	1	45	2.3	1.3	43.48	4573	0.22	0.01	Loss of cyclable lithium with slight loss of graphite active material	[38]
5	$LiFePO_4$ (LFP)	Graphite	LiPF6 in EC-DMC	1	25	1.06	1	5.66	5	12.00	1.13	Loss of cyclable lithium	[39]
6	$LiFePO_4$ (LFP)	Graphite	LiPF6 in EC-DMC	1	40	1.06	0.92	13.21	5	28.00	2.64	Loss of cyclable lithium and platting occurred	[39]
7	$LiFePO_4$ (LFP)	Graphite	LiPF6 in EC-DMC	1	55	1.06	0.75	29.25	5	62.00	5.85	Loss of cyclable lithium and SEI layer growth	[39]
8	$LiFePO_4$ (LFP)	C6	LiPF6 in solution	1	20	2.3	2.2	4.35	400	0.25	0.01	Loss of cyclable lithium	[40]

`	$LiFePO_4$ (LFP)	C6	LiPF6 in solution	1	40	2.3	2.15	6.52	300	0.50	0.02	Loss of cyclable lithium and SEI layer growth	[40]
10	$LiFePO_4$ (LFP)	C6	LiPF6 in solution	1	60	0.9	0.5	44.44	300	1.33	0.15	Gas generation occurred	[40]
11	$LiFePO_4$ (LFP)	Graphite	LiPF6 in solution	1	30	2.3	2.15	6.52	500	0.30	0.01	Loss of cyclable lithium due to SEI layer growth	[41]
12	$LiFePO_4$ (LFP)	Graphite	LiPF6 in solution	1	45	2.25	2.06	8.44	500	0.38	0.02	Loss of cyclable lithium due to SEI layer growth	[41]
13	$LiFePO_4$ (LFP)	Graphite	LiPF6 in solution	1	60	2.25	1.95	13.33	500	0.60	0.03	Loss of cyclable lithium due to SEI layer growth	[41]
14	$LiFePO_4$ (LFP)	Graphite	LiPF6 in solution	2	25	2.3	2.08	9.57	500	0.44	0.02	Loss of cyclable lithium due to SEI layer growth	[41]
15	$LiFePO_4$ (LFP)	Graphite	LiPF6 in solution	2	25	2.3	2.25	2	350	0.13	0.01	Loss of cyclable lithium	[42]
16	$LiFePO_4$ (LFP)	Graphite	LiPF6 in mixture of DEC and EC	3	25	101.99*	71.02*	30.37	300		0.10	LFP material expansion/contraction	[43]
17	$LiFePO_4$ (LFP)	Graphite	LiPF6 in mixture of DEC and EC	3	55	148.02*	55.96*	62.19	300		0.21	LFP material expansion/contraction	[43]
18	$LiNiMnCoO_2$ (NMC)	Graphite	Solution of LiPF6	1	45	4	3.2	20	100	8	0.2	Increase amounts of lithium platting occurred during cycling	[44]

19	$LiNiMnCoO_2$ (NMC)	Graphite	Solution of LiPF6	1	65	4	2	50	100	20	0.5	Growth of thick and more resistive SEI layer on graphite electrodes	[44]
20	$LiNiMnCoO_2$ (NMC333)	Graphite	LiPF6 in EC-EMC	0.33	80	1.2	0.005	99.58	100	11.95	1.00	Large resistance increases with the growth, dominantly cathode related	[45]
21	$LiNiMnCoO_2$ (NMC333)	Graphite	LiPF6 in organic solution	2	10	1.2	0.95	20.83	4500	0.056	0.0046	Loss of cyclable lithium due to SEI layer growth	[46]
22	$LiNiMnCoO_2$ (NMC333)	Graphite	LiPF6 in organic solution	2	34	1.5	1.3	13.33	5000	0.04	0.0027	Loss of cyclable lithium	[46]
23	$LiNiMnCoO_2$ (NMC333)	Graphite	LiPF6 in organic solution	2	46	0.85	0.6	29.41	2000	0.13	0.0147	Loss of cyclable lithium and loss of active material	[46]
24	$LiNiMnCoO_2$ (NMC333)	Graphite	LiPF6 in DC-DMC	1	30	1.6	1.4	12.5	100	2	0.125		[47]
25	$LiNiMnCoO_2$ (NMC622)	Graphite	LiPF6 in EC-EMC + 2 wt% VC	1	40	3.15	2.9	7.94	500	0.5	0.0159	Loss of lithium inventory due to growth of SEI and lithium plating	[48]
26	$LiNiMnCoO_2$ (NMC622)	Graphite	LiPF6 in EC-EMC + 2 wt% VC	1	25	3.13	2.85	8.95	500	0.56	0.018	Loss of lithium inventory due to growth of	[48]

												SEI and lithium plating	
27	$LiNiMnCoO_2$ (NMC622)	Graphite	LiPF6 in EC-EMC + 2 wt% VC	1	0	2.13	1.95	8.45	500	0.36	0.017	Loss of lithium inventory due to growth of SEI and lithium plating	[48]
28	$LiNiMnCoO_2$ (NMC622)	Graphite	LiPF6 in EC-EMC + 2 wt% VC	1	-10	1.35	1.3	3.70	500	0.1	0.0074	Loss of lithium inventory due to growth of SEI and lithium plating	[48]
29	$LiNiMnCoO_2$ (NMC532)	Graphite	LiPF6 in EC-DEC-DMC	0.33	25	191.2*	166.9*	12.71	100		0.13	Formation of unstable SEI layer due to catalytic activity of Ni^{4+}	[49]
30	$LiNiMnCoO_2$ (NMC532)	Graphite	LiPF6 in EC-DEC-DMC	0.33	55	173.3*	133.4*	23.02	100		0.23	Formation of unstable SEI layer due to catalytic activity of Ni^{4+}	[49]
31	$LiNiMnCoO_2$ (NMC532)	Lithium metal	LiPF6 in EC-DMC-EMC	1	25	186.6*	138.3*	25.88	100		0.26	Reduction of coulomb efficiency due to erratic Ni^{4+}	[50]
32	$LiNiMnCoO_2$ (NMC811)	Lithium metal	LiPF6 in DMC-EC-DEC	1	25	171.8*	135.6*	21.07	100		0.21		[51]
33	$LiNiMnCoO_2$ (NMC811)	Lithium metal	LiPF6 in DMC-EC-DEC	2	25	163.8*	119.4*	27.11	100		0.27		[51]

34	$LiNiMnCoO_2$ (NMC811)	Lithium metal	LiPF6 in DMC-EC-DEC	5	25	147.1*	95.76*	34.90	100		0.35		[51]
35	$LiNiMnCoO_2$ (NMC333)	Lithium metal	LiPF6 in EC-DEC	1	25	171*	155.61*	9	100		0.09		[52]
36	$LiNiMnCoO_2$ (NMC333)	Lithium metal	LiPF6 in EC-DEC	1	55	149*	105*	29.53	100		0.30		[52]
37	$LiNiMnCoO_2$ (NMC532)	Graphite	LiPF6 in EC-DMC-EMC	0.2	25	2.03	0.82	59.61	500	2.42	0.119	Loss of cyclable lithium due to SEI layer formation	[53]
38	$LiNiMnCoO_2$ (NMC532)	Graphite	LiPF6 in EC-DMC-EMC	1	25	1.9	0.37	80.53	500	3.06	0.16	Loss of cyclable lithium due to SEI layer formation	[53]
39	$LiNiMnCoO_2$ (NMC333)	Lithium metal	LiPF6 in EC-DEC	0.5	25	145	140	3.45	100		0.034		[54]
40	$LiNiMnCoO_2$ (NMC333)	Lithium metal	LiPF6 in EC-DEC	0.5	55	162.3*	150*	7.58	100		0.076		[54]
41	$LiNiMnCoO_2$ (NMC532)	Lithium metal	LiPF6 in EC-DEC	0.5	25	165.4*	156.8*	5.20	100		0.052		[54]
42	$LiNiMnCoO_2$ (NMC532)	Lithium metal	LiPF6 in EC-DEC	0.5	55	176.6*	158.9*	10.02	100		0.10		[54]
43	$LiNiMnCoO_2$ (NMC622)	Lithium metal	LiPF6 in EC-DEC	0.5	25	172.1*	159.5*	7.32	100		0.073		[54]
44	$LiNiMnCoO_2$ (NMC622)	Lithium metal	LiPF6 in EC-DEC	0.5	55	184.3*	156.84*	14.90	100		0.15		[54]
45	$LiNiMnCoO_2$ (NMC811)	Lithium metal	LiPF6 in EC-DEC	0.5	25	192.8*	155.1*	19.55	100		0.20		[54]
46	$LiNiMnCoO_2$ (NMC811)	Lithium metal	LiPF6 in EC-DEC	0.5	55	205.8*	144.47*	29.80	100		0.30		[54]

*Cells in green have units of mAh g^{-1}

Appendix B: Data of Initial Capacity of NMC811 and LFP

No.	Cathode	Anode	Electrolyte	C-Rate	T (°C)	Initial Capacity (mAh/g)	References
1	LiFePO4 (LFP)	Graphite	LiPF6 in mixture of DEC and EC	0.2	25	150	[43]
2	LiFePO4 (LFP)	Graphite	LiPF6 in mixture of DEC and EC	1	25	135	[43]
3	LiFePO4 (LFP)	Graphite	LiPF6 in mixture of DEC and EC	10	25	90	[43]
4	LiNiMnCoO2 (NMC811)	Lithium metal	LiPF6 in DMC-EC-DEC	1	25	171.8	[51]
5	LiNiMnCoO2 (NMC811)	Lithium metal	LiPF6 in DMC-EC-DEC	2	25	163.8	[51]
6	LiNiMnCoO2 (NMC811)	Lithium metal	LiPF6 in DMC-EC-DEC	5	25	147.1	[51]

Table 3 Data of Initial Capacity of NMC811 and LFP